

FANoS: Friction-Adaptive Nosé–Hoover Symplectic Momentum for Stiff Objectives

Nalin Dhiman

*School of Computing and Electrical Engineering
Indian Institute of Technology, Mandi, India
d24008@students.iitmandi.ac.in*

Abstract

We study a physics-inspired optimizer, *FANoS* (Friction-Adaptive Nosé–Hoover Symplectic momentum), which combines (i) a momentum update written as a discretized second-order dynamical system, (ii) a Nosé–Hoover-like thermostat variable that adapts a scalar friction coefficient using kinetic-energy feedback, and (iii) a semi-implicit (symplectic-Euler) integrator, optionally with a diagonal RMS preconditioner. The method is motivated by structure-preserving integration and thermostat ideas from molecular dynamics, but is used here purely as an optimization heuristic.

We provide the algorithm and limited theoretical observations in idealized settings. On the deterministic Rosenbrock-100D benchmark with 3000 gradient evaluations, FANoS-RMS attains a mean final objective value of 1.74×10^{-2} , improving substantially over unclipped AdamW (48.50) and SGD+momentum (90.76) in this protocol. However, AdamW with gradient clipping is stronger, reaching 1.87×10^{-3} , and L-BFGS reaches $\approx 4.4 \times 10^{-10}$. On ill-conditioned convex quadratics and in a small PINN warm-start suite (Burgers and Allen–Cahn), the default FANoS configuration underperforms AdamW and can be unstable or high-variance.

Overall, the evidence supports a conservative conclusion: FANoS is an interpretable synthesis of existing ideas that can help on some stiff nonconvex valleys, but it is not a generally superior replacement for modern baselines, and its behavior is sensitive to temperature-schedule and hyperparameter choices.

1 Introduction

Gradient-based training is usually framed as optimization, but it is also numerical integration: we repeatedly apply discrete update rules that approximate some continuous-time dynamics. When an objective has directions with widely separated curvature scales (“stiffness”), naive discretizations can exhibit instability, energy drift, or slow progress along narrow valleys. These phenomena are familiar in scientific computing and molecular dynamics, where *structure-preserving* integrators and *thermostats* are used to reduce long-time energy drift and to regulate kinetic energy [10, 4, 3].

This paper asks a narrow question: can a simple Nosé–Hoover-inspired feedback variable (a learned friction coefficient) and a symplectic (semi-implicit) momentum discretization be a useful optimizer component on stiff objective landscapes? We study FANoS, a friction-adaptive symplectic momentum method that introduces a scalar thermostat variable to adjust friction online, with the goal of regulating the kinetic energy of the momentum state. FANoS also permits a diagonal RMS-type “mass” (preconditioner) reminiscent of RMSProp [15].

What this paper is (and is not). We do *not* claim a new state-of-the-art general-purpose optimizer. We do *not* claim nonconvex convergence guarantees. Instead, we aim for an honest, reproducible study of a specific synthesis: Nosé–Hoover-style feedback + symplectic discretization + optional diagonal preconditioning. We emphasize strong baselines (including gradient clipping) and we report negative results where they occur.

Contributions.

- We present FANoS as a concrete optimizer and describe its implementation, including a semi-implicit (symplectic-Euler) discretization and a kinetic-energy feedback thermostat.
- We provide limited theoretical analysis in idealized settings, clarifying why symplectic updates can avoid the immediate energy blow-up of explicit Euler on oscillatory (stiff) modes.
- We report a reproducible evaluation suite (code + logs packaged with this draft) on (i) Rosenbrock-100D learning-rate sweeps, (ii) a diagnostic ill-conditioned quadratic sweep, and (iii) a PINN warm-start suite. The evaluation includes bootstrap confidence intervals and divergence rates.

2 Related work

Momentum and adaptive first-order methods. Classical momentum methods (heavy-ball, Nesterov acceleration) can be interpreted as discretizations of second-order dynamics [12, 8]. Modern adaptive optimizers (Adam, RMSProp, AdamW) introduce coordinate-wise learning-rate normalization and bias corrections [5, 15, 7].

Second-order and quasi-Newton methods. On deterministic objectives, quasi-Newton methods such as L-BFGS can converge rapidly [6, 9]. Their use at scale in stochastic mini-batch regimes is less direct and can be computationally expensive.

Thermostats and stochastic-gradient MCMC. Nosé–Hoover thermostats control temperature in molecular dynamics [10, 4]. Related ideas appear in stochastic-gradient MCMC, e.g., SGNHT [2], which adds auxiliary variables to stabilize momentum under gradient noise. FANoS is *not* a sampler; it borrows the thermostat control idea as an optimization heuristic.

Geometric integration. Symplectic methods are designed to control long-term energy drift in Hamiltonian systems [3]. In optimization, using symplectic discretizations is less common but can be motivated when an update resembles a mechanical system (position + velocity).

3 FANoS: dynamics and discrete algorithm

Let $f(\theta)$ be an objective with parameters $\theta \in \mathbb{R}^d$ and gradient $g(\theta) = \nabla f(\theta)$. We introduce an auxiliary velocity $v \in \mathbb{R}^d$ and a scalar friction variable $\zeta \in \mathbb{R}$.

3.1 Continuous-time motivation (idealized)

A simplified controlled dynamics can be written as

$$\dot{\theta} = v, \quad (1)$$

$$\dot{v} = -M(\theta)^{-1}g(\theta) - \zeta v, \quad (2)$$

$$\dot{\zeta} = \frac{1}{Q}(T(v; M) - T_0(t)), \quad (3)$$

where $M(\theta) \succ 0$ acts as a mass (preconditioner), $Q > 0$ is a thermostat inertia, $T_0(t) \geq 0$ is a target kinetic-energy level, and

$$T(v; M) = \frac{1}{d}v^\top M v \quad (4)$$

is a kinetic-energy proxy. In this view, ζ is an *integral controller*: if kinetic energy exceeds the target, ζ increases, adding damping; if kinetic energy is below target, ζ can decrease (even becoming negative), reducing damping and potentially injecting energy.

Remark 1 (Scope of the continuous-time view). *Equations (2)–(3) are not claimed as an exact limit of SGD. In stochastic training, mini-batch gradients add noise; SG-MCMC methods include additional diffusion terms for sampling guarantees [16, 1, 2]. We use (2)–(3) only as an organizing principle for the discrete optimizer.*

3.2 Discrete update (implemented)

FANoS uses a semi-implicit (symplectic-Euler-style) discretization for the (θ, v) update and a discrete thermostat update for ζ . We also include a diagonal RMS preconditioner via an exponential moving average of squared gradients. Let $h > 0$ denote the step size (we use $h = 1\text{r}$). For each coordinate i :

$$s_{k+1,i} \leftarrow \beta s_{k,i} + (1 - \beta)g_{k,i}^2, \quad (5)$$

$$m_{k+1,i} \leftarrow \sqrt{s_{k+1,i}} + \varepsilon, \quad (6)$$

$$v_{k+1,i} \leftarrow (1 - h\zeta_k)v_{k,i} - h\frac{g_{k,i}}{m_{k+1,i}}, \quad (7)$$

$$\theta_{k+1,i} \leftarrow \theta_{k,i} + hv_{k+1,i}. \quad (8)$$

The identity-mass variant sets $m_{k+1,i} \equiv 1$.

The thermostat uses a group-level kinetic-energy estimate

$$T_{\text{inst}} \leftarrow \frac{1}{d} \sum_{i=1}^d m_{k+1,i} v_{k+1,i}^2, \quad (9)$$

$$T_{\text{ema}} \leftarrow \rho_T T_{\text{ema}} + (1 - \rho_T) T_{\text{inst}}, \quad (10)$$

$$\zeta_{k+1} \leftarrow \text{clip}\left(\zeta_k + \frac{h}{Q}(T_{\text{ema}} - T_0(k)), [-\zeta_{\max}, \zeta_{\max}]\right). \quad (11)$$

We use an exponential target schedule

$$T_0(k) = T_{\min} + (T_{\max} - T_{\min}) \exp(-k/\tau). \quad (12)$$

Hyperparameters in the released implementation. Unless otherwise stated, FANoS uses $\beta = 0.999$, $\varepsilon = 10^{-8}$, $Q = 1$, $T_{\max} = 10^{-3}$, $T_{\min} = 0$, $\tau = 20000$, $\rho_T = 0.9$, and $\zeta_{\max} = 10$. We use global gradient norm clipping with threshold $c = 1$ by default.

Algorithm 1 FANoS (one parameter group; diagonal mass; semi-implicit update)

Require: step size h , EMA parameter β, ε , thermostat inertia Q , target schedule $T_0(k)$, temperature EMA ρ_T , clip bound ζ_{\max} , optional grad clip c

- 1: Initialize $v \leftarrow 0, s \leftarrow 0, \zeta \leftarrow 0, T_{\text{ema}} \leftarrow T_{\max}$
- 2: **for** $k = 0, 1, 2, \dots$ **do**
- 3: $g \leftarrow \nabla f(\theta_k)$
- 4: **if** grad clip enabled **then**
- 5: $g \leftarrow g \cdot \min\{1, c/(\|g\| + 10^{-12})\}$
- 6: **end if**
- 7: $s \leftarrow \beta s + (1 - \beta)g \odot g$
- 8: $m \leftarrow \sqrt{s} + \varepsilon$
- 9: $v \leftarrow (1 - h\zeta)v - h g \oslash m$
- 10: $\theta \leftarrow \theta + h v$ ▷ semi-implicit / symplectic Euler
- 11: $T_{\text{inst}} \leftarrow \frac{1}{d} \sum_i m_i v_i^2$
- 12: $T_{\text{ema}} \leftarrow \rho_T T_{\text{ema}} + (1 - \rho_T)T_{\text{inst}}$
- 13: $\zeta \leftarrow \text{clip}\left(\zeta + \frac{h}{Q}(T_{\text{ema}} - T_0(k)), [-\zeta_{\max}, \zeta_{\max}]\right)$
- 14: **end for**

Gradient clipping. Gradient clipping is a standard stabilizer in deep learning [11]. We treat it as a baseline component: when FANoS uses clipping, we also report “+clip” variants of AdamW and RMSProp in the Rosenbrock sweep.

3.3 Algorithm

Algorithm 1 summarizes the implemented algorithm for one parameter group.

4 Theory in a simplified setting

This section provides two limited but useful facts: (i) symplectic Euler can avoid the immediate energy blow-up of explicit Euler on oscillatory modes, and (ii) the thermostat update can be interpreted as integral feedback on kinetic energy. These statements do not imply global convergence for nonconvex stochastic training.

4.1 Why semi-implicit updates can help stability

Consider the one-dimensional quadratic $f(x) = \frac{1}{2}\omega^2 x^2$ with gradient $g(x) = \omega^2 x$. The undamped second-order dynamics

$$\dot{x} = v, \quad \dot{v} = -\omega^2 x \tag{13}$$

is a harmonic oscillator with frequency ω . Stiffness corresponds to large ω .

Theorem 1 (Linear stability of symplectic Euler on the harmonic oscillator). *Apply the semi-implicit update*

$$v_{k+1} = v_k - h\omega^2 x_k, \quad x_{k+1} = x_k + hv_{k+1}. \tag{14}$$

The update matrix has determinant 1 and eigenvalues on the unit circle when $0 < h\omega < 2$. In contrast, explicit Euler applied to the same system yields an update matrix with spectral radius strictly greater than 1 for any $h > 0$.

Proof. The semi-implicit update can be written as

$$\begin{pmatrix} x_{k+1} \\ v_{k+1} \end{pmatrix} = \begin{pmatrix} 1 - h^2\omega^2 & h \\ -h\omega^2 & 1 \end{pmatrix} \begin{pmatrix} x_k \\ v_k \end{pmatrix} =: A \begin{pmatrix} x_k \\ v_k \end{pmatrix}.$$

A direct computation gives $\det(A) = 1$ and $\text{tr}(A) = 2 - h^2\omega^2$. The eigenvalues satisfy $\lambda + \lambda^{-1} = \text{tr}(A)$. Thus $|\lambda| = 1$ iff $|\text{tr}(A)| < 2$, i.e., $0 < h^2\omega^2 < 4$.

For explicit Euler, $x_{k+1} = x_k + hv_k$, $v_{k+1} = v_k - h\omega^2 x_k$ corresponds to $A_{\text{EE}} = \begin{pmatrix} 1 & h \\ -h\omega^2 & 1 \end{pmatrix}$ with $\det(A_{\text{EE}}) = 1 + h^2\omega^2 > 1$, so the spectral radius exceeds 1 for any $h > 0$. \square

Remark 2 (Interpretation). *Theorem 1 illustrates a basic mechanism: for oscillatory directions, a symplectic discretization can preserve bounded energy over a range of step sizes where explicit Euler explodes. This does not guarantee better optimization performance, but it motivates the semi-implicit choice in FANoS.*

4.2 Thermostat as feedback on kinetic energy

Let $T(v; M) = \frac{1}{d}v^\top M v$ and suppose for intuition that M is constant and gradients are noise-free. Then (3) increases ζ when T is above T_0 and decreases it otherwise. In discrete time, the update

$$\zeta_{k+1} = \zeta_k + \frac{h}{Q} (T_{\text{ema}} - T_0(k))$$

is an integral controller (with smoothing via T_{ema}). The clip bound ζ_{max} prevents extreme friction (positive or negative) caused by transient gradient spikes.

4.3 Overdamped intuition: connection to preconditioned gradient descent

If ζ is large and positive in (2), then v relaxes quickly to a quasi-steady state $v \approx -\zeta^{-1}M^{-1}g(\theta)$. Substituting into $\dot{\theta} = v$ yields a preconditioned gradient flow

$$\dot{\theta} \approx -\frac{1}{\zeta} M^{-1}g(\theta), \quad (15)$$

so the friction level ζ acts as an adaptive global inverse step-size. This heuristic helps interpret why the thermostat variable can strongly affect effective learning rate, and why a poorly matched $T_0(k)$ schedule can lead to slow or non-convergent behavior on simple convex problems.

5 Experimental protocol

All experiments are implemented in PyTorch and run on CPU. Each benchmark uses multiple random seeds and reports mean performance with a bootstrap confidence interval (CI) across seeds. We report *final objective values* at a fixed evaluation budget, rather than best-over-time, to keep the protocol simple and reproducible.

5.1 Rosenbrock-100D learning-rate sweep

We use the Rosenbrock function [14] in dimension $d = 100$:

$$f(\theta) = \sum_{i=1}^{d-1} [100(\theta_{i+1} - \theta_i^2)^2 + (1 - \theta_i)^2]. \quad (16)$$

Initialization is $\theta_i \sim \mathcal{U}[-2, 2]$ with a fixed seed. We run 3000 gradient evaluations per trial and sweep learning rates

$$h \in \{10^{-4}, 10^{-3}, 3 \cdot 10^{-3}, 10^{-2}, 3 \cdot 10^{-2}, 10^{-1}\}.$$

We report results for SGD with momentum (SGD+Mom), AdamW, RMSProp, L-BFGS, FANoS-RMS, plus clipped variants AdamW+clip and RMSProp+clip. Clipping uses a global norm threshold $c = 1$.

Baseline hyperparameters (as in the released scripts). Unless otherwise stated, baselines use PyTorch defaults. SGD+Mom uses momentum 0.9. AdamW uses $\beta_1 = 0.9$, $\beta_2 = 0.999$, $\varepsilon = 10^{-8}$, and PyTorch’s default weight decay (0.01). RMSProp uses $\alpha = 0.99$ and $\varepsilon = 10^{-8}$ with zero momentum. L-BFGS uses history size 100 with `strong_wolfe` line search, and is constrained to the same evaluation budget by counting objective/gradient evaluations inside the closure. For the “+clip” variants, we apply global gradient norm clipping with threshold $c = 1$ each step.

Caveat (weight decay on synthetic objectives). Weight decay is not an intrinsic part of Rosenbrock optimization and can shift the effective objective. We keep the AdamW default because it is the setting actually used to generate the attached results; the comparison should therefore be read as a comparison between these specific optimizer configurations.

5.2 Ill-conditioned quadratic sweep (diagnostic)

We generate convex quadratics $f(x) = \frac{1}{2}x^\top Ax$ in $d = 100$ with a random orthogonal eigenbasis and log-spaced eigenvalues spanning a prescribed condition number $\kappa(A) \in \{10^2, 10^3, 10^4, 10^5, 10^6\}$. Each setting uses 3000 gradient evaluations and three random seeds. Learning rates are fixed per method (no per- κ tuning in this diagnostic).

Learning rates in this diagnostic are fixed per method as follows: SGD+Mom 10^{-3} , RMSProp 10^{-3} , AdamW 10^{-2} , L-BFGS 10^{-1} , FANoS-RMS 10^{-3} . AdamW again uses PyTorch default weight decay (0.01) in the released script.

5.3 PINN warm-start suite (Burgers, Allen–Cahn)

We evaluate a small physics-informed neural network (PINN) setup [13] for two 1D PDEs on $x \in [-1, 1]$, $t \in [0, 1]$:

- Viscous Burgers: $u_t + uu_x - \nu u_{xx} = 0$ with $\nu = 0.01/\pi$ and initial condition $u(x, 0) = -\sin(\pi x)$.
- Allen–Cahn (as implemented): $u_t - \nu u_{xx} + 5u^3 - 5u = 0$ with $\nu = 10^{-4}$.

We use a fully-connected network with tanh activations (architecture [2, 50, 50, 50, 1]). For each problem and seed, we run a warm-start phase of 1000 steps with AdamW, RMSProp, or FANoS (all at learning rate 10^{-3}), followed by L-BFGS refinement (PyTorch L-BFGS, `max_iter = 200`). We report warm-start loss and post-LBFGS loss.

Warm-start hyperparameters for AdamW and RMSProp are PyTorch defaults (in particular, AdamW uses default weight decay 0.01). FANoS uses the hyperparameters listed in the method section, with learning rate 10^{-3} for warm-start.

6 Results

This section reports the results exactly as produced by the attached results package. We highlight both positive and negative outcomes.

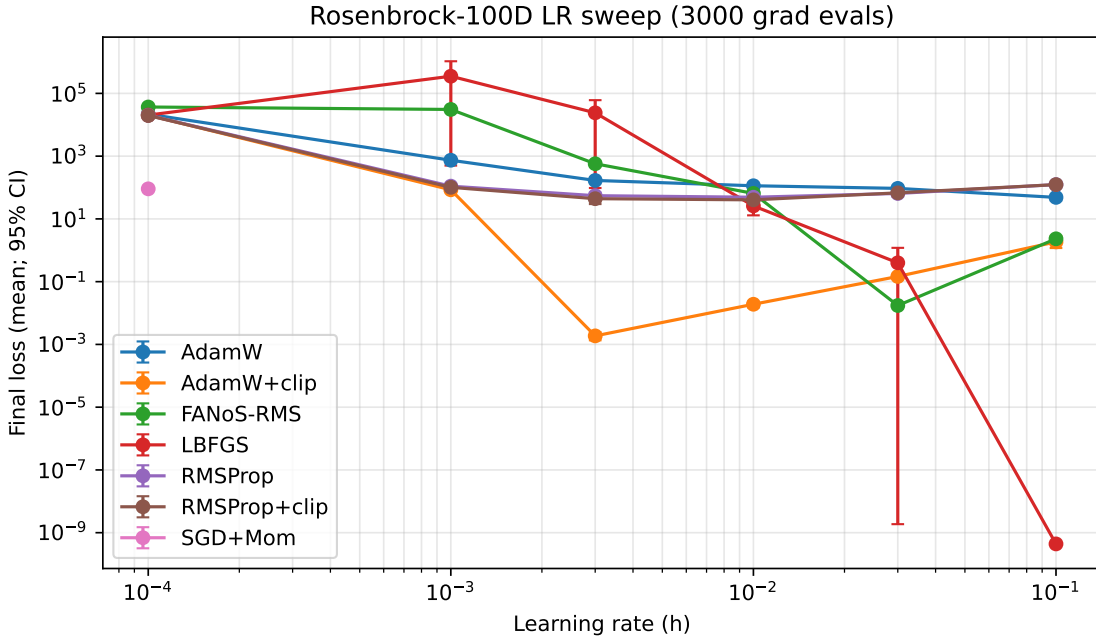


Figure 1: Rosenbrock-100D learning-rate sweep (mean final loss; 95% bootstrap CI; 10 seeds; 3000 gradient evaluations).

6.1 Rosenbrock-100D: FANO-S helps vs unclipped baselines, but not vs AdamW+clip

Figure 1 shows the learning-rate sweep, and Table 1 summarizes the best learning rate (by mean final loss) for each method. FANO-S-RMS achieves a mean final loss of 1.74×10^{-2} at $h = 3 \times 10^{-2}$, substantially improving over the unclipped AdamW and RMSProp baselines under the same evaluation budget. However, AdamW with gradient clipping attains a lower loss ($\approx 1.87 \times 10^{-3}$) under this protocol. L-BFGS reaches near machine precision, as expected for a deterministic smooth objective.

6.2 Quadratic sweep: default FANO-S configuration performs poorly in this diagnostic

Figure 2 and Table 2 report the ill-conditioned quadratic sweep. Under the fixed learning-rate choices used in this diagnostic, FANO-S-RMS yields substantially larger final losses than the other methods across all tested condition numbers. This negative result suggests that the default thermostat schedule and hyperparameters (notably the target temperature decay time scale) are not appropriate for this short-budget convex setting.

6.3 PINN warm-start suite: FANO-S underperforms AdamW in this configuration

Figure 3 reports final losses after L-BFGS refinement for the two PDE problems. In this suite, FANO-S warm-start is worse than AdamW warm-start for Burgers and substantially worse (with high variance) for Allen–Cahn. These results do *not* support a claim that FANO-S is a generally useful warm-start for PINN training, at least under the shared hyperparameters used here.

Method	Best LR	Mean loss	Std	95% CI	Div. rate
AdamW	0.1	48.4967	15.4426	[39.2351, 57.9358]	0%
AdamW+clip	0.003	1.87e-03	8.91e-04	[1.35e-03, 2.44e-03]	0%
FANoS-RMS	0.03	0.0174	2.74e-03	[0.0157, 0.0191]	0%
LBFGS	0.1	4.39e-10	2.11e-11	[4.25e-10, 4.51e-10]	0%
RMSProp	0.01	49.0644	22.0357	[34.5316, 61.8801]	0%
RMSProp+clip	0.01	40.4506	20.9825	[26.3367, 52.6370]	0%
SGD+Mom	0.0001	90.7630	15.0678	[82.7020, 101.3934]	0%

Table 1: Rosenbrock-100D: best learning rate per method (mean final loss; 95% bootstrap CI; 10 seeds).

6.4 Thermostat diagnostics: kinetic energy may not track the target without tuning

Figure 4 shows thermostat diagnostics recorded during Rosenbrock training for two learning-rate regimes (“Good” and “Bad” as labeled by the diagnostics script). In both regimes, the kinetic-energy proxy T_{inst} and its EMA T_{ema} deviate from the target T_0 , while the friction variable ζ drifts upward. Under the tested hyperparameters, the thermostat therefore acts more like a slowly varying damping term than a tight temperature regulator. This diagnostic is useful for debugging and for guiding tuning (e.g., changing Q , τ , ρ_T , or the definition of T).

7 Discussion and limitations

A narrow positive result. In Rosenbrock-100D, FANoS-RMS substantially improves over unclipped AdamW/RMSProp under the fixed-budget protocol. This suggests that friction-adaptive momentum combined with RMS-style scaling can help on some stiff nonconvex valleys.

Clipping is a strong baseline. Gradient clipping makes AdamW dramatically stronger on Rosenbrock, outperforming FANoS-RMS. Because FANoS uses clipping internally in this package, comparisons to clipped baselines are essential. Any claim about optimizer superiority is contingent on baseline choices and stabilizers.

Observed failure modes. The quadratic sweep and PINN suite indicate that the released FANoS configuration is not robust across problem classes. A plausible explanation is hyperparameter mismatch: if the target temperature $T_0(k)$ decays too slowly relative to the evaluation budget, FANoS can behave like a permanently “heated” method that does not settle near the minimizer on convex problems. PINNs also exhibit well-known sensitivity to optimizer settings and loss design [13]. The thermostat diagnostics further suggest that the implemented temperature feedback does not tightly regulate kinetic energy for the chosen Q and ρ_T .

Computational overhead. FANoS introduces additional state $(v, s, \zeta, T_{\text{ema}})$ and a small amount of extra computation per step (mass update + thermostat update). We do not claim an efficiency advantage.

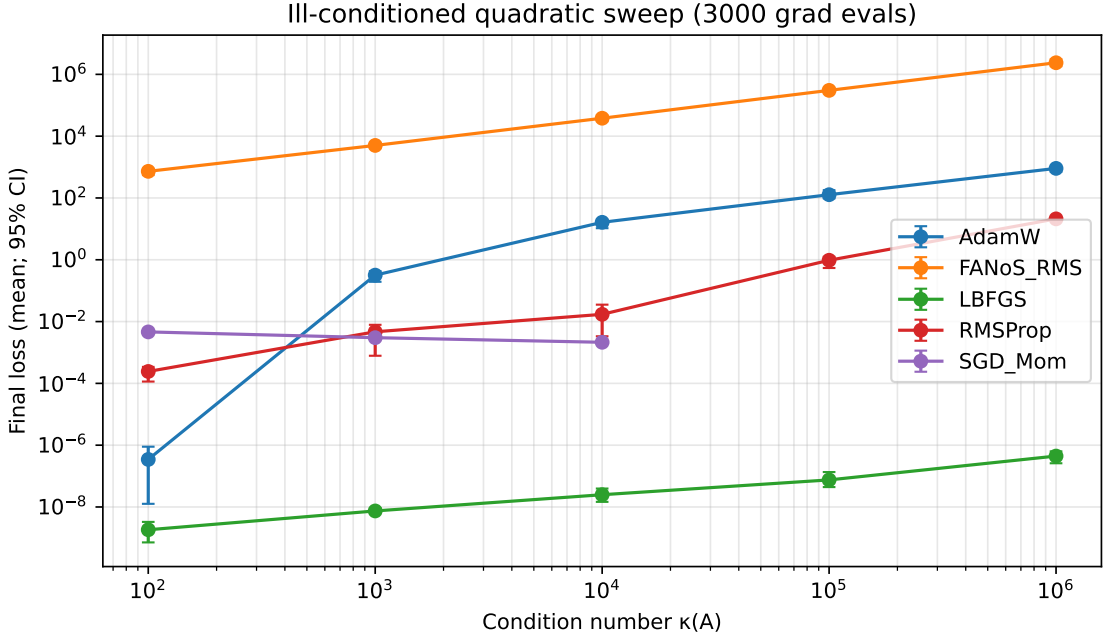


Figure 2: Ill-conditioned quadratic sweep (mean final loss; 95% bootstrap CI; 3 seeds; 3000 gradient evaluations). Learning rates are fixed per method (no tuning per condition number).

No general-purpose claim. We do not claim that FANoS is competitive with AdamW on standard vision/NLP benchmarks, nor do we present GPU-scale training results. The current evidence supports only benchmark-specific statements on stiff deterministic landscapes.

8 Conclusion

FANoS is a physics-inspired optimizer that combines a Nosé–Hoover-like friction controller with a semi-implicit (symplectic) momentum update and optional RMS-style diagonal scaling. Our reproducible evaluation yields a mixed picture: FANoS improves over some unclipped baselines on Rosenbrock-100D but is outperformed by AdamW with gradient clipping under the same budget, and it performs poorly on ill-conditioned convex quadratics and in a small PINN warm-start suite under the tested configuration. Thermostat diagnostics indicate imperfect kinetic-energy tracking without careful tuning. These findings suggest that FANoS is best viewed as an interpretable research direction and a potentially useful tool in select stiff nonconvex regimes, rather than a drop-in replacement for established optimizers. [Code is available at: Github](#)

Method	κ	Mean loss	Std	95% CI	Div. rate
AdamW	1e+02	3.46e-07	3.90e-07	[1.26e-08, 8.92e-07]	0%
FANoS_RMS	1e+02	726.7047	131.4858	[550.3011, 865.8386]	0%
LBFGS	1e+02	1.83e-09	1.08e-09	[7.14e-10, 3.29e-09]	0%
RMSProp	1e+02	2.43e-04	9.50e-05	[1.14e-04, 3.41e-04]	0%
SGD_Mom	1e+02	4.63e-03	4.35e-04	[4.01e-03, 4.94e-03]	0%
AdamW	1e+03	0.3183	0.0961	[0.1938, 0.4277]	0%
FANoS_RMS	1e+03	5.01e+03	792.4805	[4.12e+03, 6.05e+03]	0%
LBFGS	1e+03	7.44e-09	1.28e-09	[6.34e-09, 9.24e-09]	0%
RMSProp	1e+03	4.67e-03	2.93e-03	[7.83e-04, 7.85e-03]	0%
SGD_Mom	1e+03	3.01e-03	2.46e-04	[2.66e-03, 3.22e-03]	0%
AdamW	1e+04	16.2930	4.1052	[10.5094, 19.6216]	0%
FANoS_RMS	1e+04	3.81e+04	6.62e+03	[3.07e+04, 4.67e+04]	0%
LBFGS	1e+04	2.49e-08	1.06e-08	[1.46e-08, 3.95e-08]	0%
RMSProp	1e+04	0.0171	0.0134	[3.34e-03, 0.0353]	0%
SGD_Mom	1e+04	2.14e-03	1.88e-04	[1.90e-03, 2.36e-03]	0%
AdamW	1e+05	127.5533	36.5602	[96.9263, 178.9426]	0%
FANoS_RMS	1e+05	3.03e+05	3.63e+04	[2.72e+05, 3.54e+05]	0%
LBFGS	1e+05	7.51e-08	4.24e-08	[4.41e-08, 1.35e-07]	0%
RMSProp	1e+05	0.9638	0.3043	[0.5416, 1.2472]	0%
SGD_Mom	1e+05	—	—	—	100%
AdamW	1e+06	906.1441	140.4453	[707.9042, 1.02e+03]	0%
FANoS_RMS	1e+06	2.38e+06	5.20e+05	[1.84e+06, 3.08e+06]	0%
LBFGS	1e+06	4.44e-07	1.52e-07	[2.60e-07, 6.31e-07]	0%
RMSProp	1e+06	21.0706	0.8336	[20.0479, 22.0899]	0%
SGD_Mom	1e+06	—	—	—	100%

Table 2: Ill-conditioned quadratic diagnostic sweep summary.

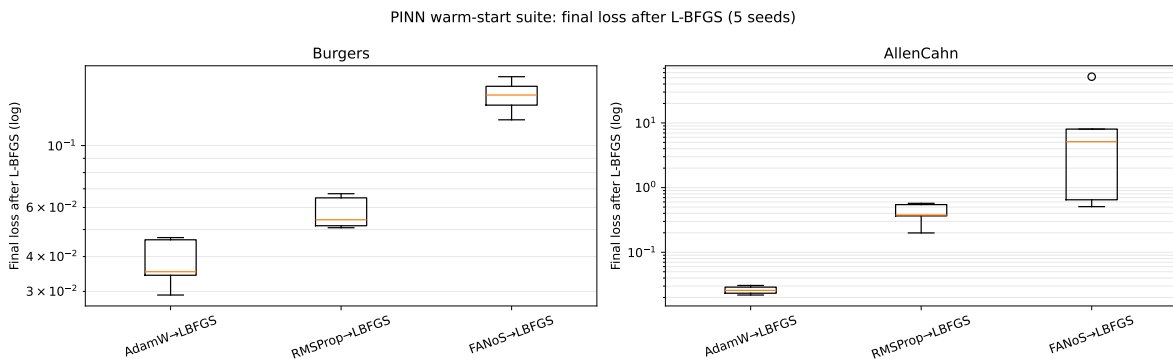


Figure 3: PINN warm-start suite: distribution of final loss after L-BFGS refinement (5 seeds). Lower is better.

Problem	Pipeline	Mean final loss	Std	95% CI	Time (mean \pm std)
AllenCahn	AdamW \rightarrow LBFGS	0.0261	3.33e-03	[0.0232, 0.0290]	34.82 \pm 3.13
AllenCahn	FANoS \rightarrow LBFGS	13.2389	19.5269	[1.4882, 32.8629]	36.78 \pm 2.54
AllenCahn	RMSProp \rightarrow LBFGS	0.4118	0.1357	[0.3012, 0.5249]	32.27 \pm 2.51
Burgers	AdamW \rightarrow LBFGS	0.0383	6.93e-03	[0.0324, 0.0442]	37.21 \pm 3.45
Burgers	FANoS \rightarrow LBFGS	0.1509	0.0183	[0.1348, 0.1665]	33.26 \pm 2.65
Burgers	RMSProp \rightarrow LBFGS	0.0577	6.94e-03	[0.0518, 0.0637]	33.37 \pm 1.55

Table 3: PINN warm-start suite: mean final loss after L-BFGS refinement and runtime (5 seeds).

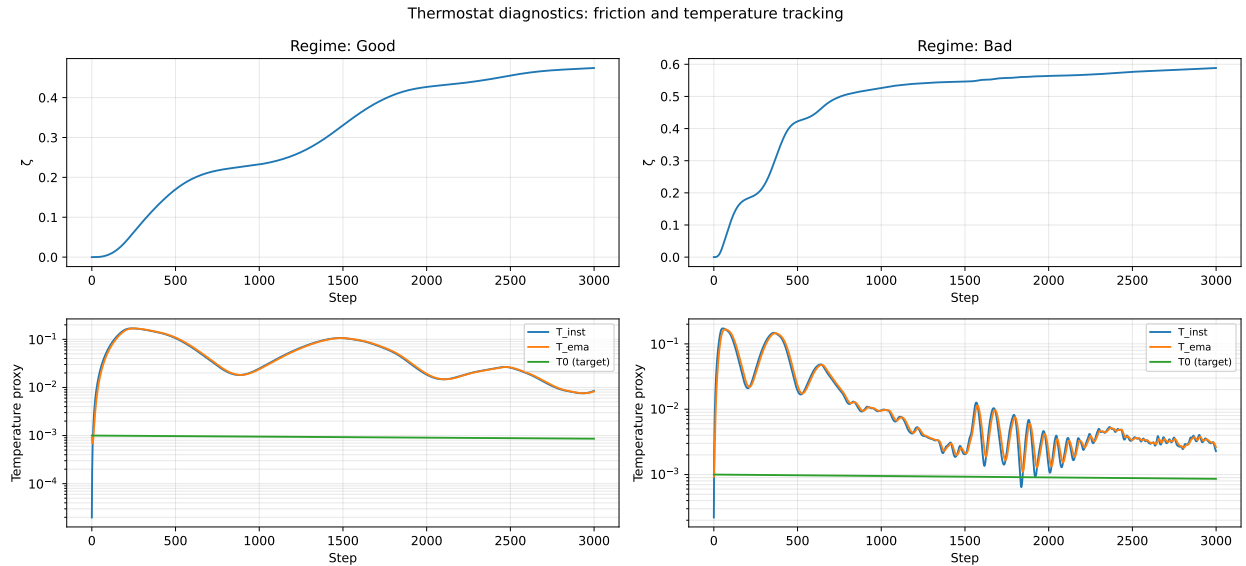


Figure 4: Thermostat diagnostics: friction coefficient ζ (top) and temperature proxies (bottom) for two Rosenbrock regimes over 3000 steps.

A Additional ablation results

We include the ablation table and plot produced by the attached pipeline for completeness. These ablations were run at a fixed learning rate passed via the ablation runner, and results can be sensitive to that choice; therefore we avoid drawing strong mechanistic conclusions from them.

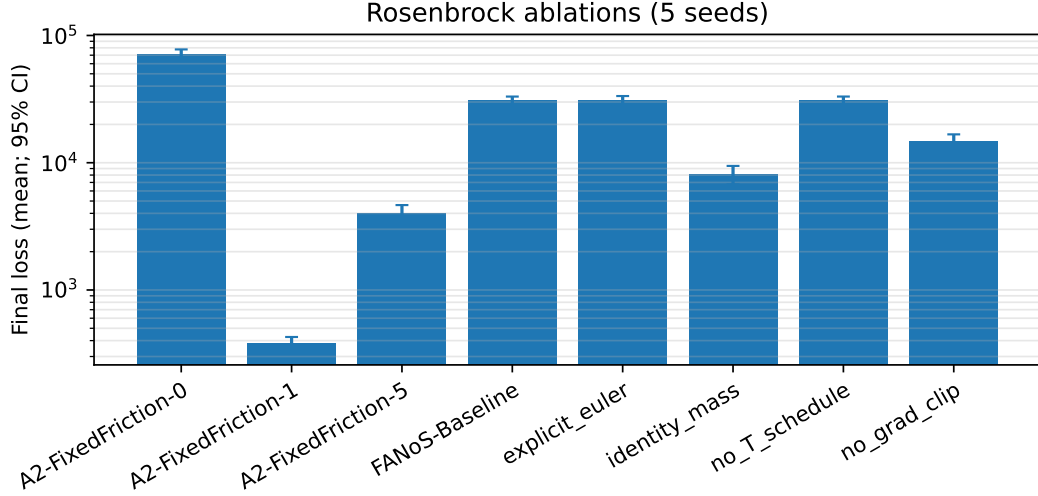


Figure 5: Rosenbrock ablations (mean final loss; 95% bootstrap CI). Interpret cautiously due to hyperparameter interactions.

Variant	Mean loss	Std	95% CI	Divergence
A2-FixedFriction-0	7.11e+04	1.09e+04	[6.39e+04, 7.77e+04]	0%
A2-FixedFriction-1	382.0143	73.2516	[338.2412, 427.1150]	0%
A2-FixedFriction-5	3.99e+03	1.08e+03	[3.31e+03, 4.65e+03]	0%
FANoS-Baseline	3.08e+04	3.90e+03	[2.83e+04, 3.31e+04]	0%
explicit_euler	3.11e+04	3.94e+03	[2.86e+04, 3.34e+04]	0%
identity_mass	8.11e+03	2.19e+03	[6.75e+03, 9.44e+03]	0%
no_T_schedule	3.08e+04	3.90e+03	[2.83e+04, 3.31e+04]	0%
no_grad_clip	1.46e+04	3.49e+03	[1.24e+04, 1.67e+04]	0%

Table 4: Rosenbrock ablation summary

References

- [1] Tianqi Chen, Emily Fox, and Carlos Guestrin. Stochastic gradient Hamiltonian monte carlo. In *International Conference on Machine Learning*, 2014.
- [2] Nan Ding, Youhan Fang, Ryan Babbush, Changyou Chen, Robert D. Skeel, and Hartmut Neven. Bayesian sampling using stochastic gradient thermostats. In *Advances in Neural Information Processing Systems*, 2014.
- [3] Ernst Hairer, Christian Lubich, and Gerhard Wanner. *Geometric Numerical Integration: Structure-Preserving Algorithms for Ordinary Differential Equations*. Springer, 2 edition, 2006.

- [4] William G. Hoover. Canonical dynamics: Equilibrium phase-space distributions. *Physical Review A*, 31(3):1695–1697, 1985.
- [5] Diederik P. Kingma and Jimmy Ba. Adam: A method for stochastic optimization. In *International Conference on Learning Representations*, 2015.
- [6] Dong C. Liu and Jorge Nocedal. On the limited memory BFGS method for large scale optimization. *Mathematical Programming*, 45(1):503–528, 1989.
- [7] Ilya Loshchilov and Frank Hutter. Decoupled weight decay regularization. In *International Conference on Learning Representations*, 2019.
- [8] Yurii Nesterov. A method for solving the convex programming problem with convergence rate $\mathcal{O}(1/k^2)$. *Soviet Mathematics Doklady*, 27:372–376, 1983.
- [9] Jorge Nocedal and Stephen J. Wright. *Numerical Optimization*. Springer, 2 edition, 2006.
- [10] Shuichi Nosé. A molecular dynamics method for simulations in the canonical ensemble. *Molecular Physics*, 52(2):255–268, 1984.
- [11] Razvan Pascanu, Tomas Mikolov, and Yoshua Bengio. On the difficulty of training recurrent neural networks. In *International Conference on Machine Learning*, 2013.
- [12] Boris T. Polyak. Some methods of speeding up the convergence of iteration methods. *USSR Computational Mathematics and Mathematical Physics*, 4(5):1–17, 1964.
- [13] Maziar Raissi, Paris Perdikaris, and George E. Karniadakis. Physics-informed neural networks: A deep learning framework for solving forward and inverse problems involving nonlinear partial differential equations. *Journal of Computational Physics*, 378:686–707, 2019.
- [14] Howard H. Rosenbrock. An automatic method for finding the greatest or least value of a function. *The Computer Journal*, 3(3):175–184, 1960.
- [15] Tijmen Tieleman and Geoffrey Hinton. Lecture 6.5—RMSProp: Divide the gradient by a running average of its recent magnitude. Technical report, University of Toronto, 2012. Technical report, Neural Networks for Machine Learning (Coursera).
- [16] Max Welling and Yee Whye Teh. Bayesian learning via stochastic gradient Langevin dynamics. In *International Conference on Machine Learning*, 2011.